



Fermi National Accelerator Laboratory

FERMILAB-Conf-95/115-E

CDF

Photon and Diphoton Production at CDF and D0

Jodi I. Lamoureux

*Fermi National Accelerator Laboratory
P.O. Box 500, Batavia, Illinois 60510*

*Brandeis University
Waltham, Massachusetts 02254*

May 1995

Presented at the *QCD and High Energy Hadronic Interactions Session of the XXXth Rencontres de Moriond*, March 19-26, 1995

Disclaimer

This report was prepared as an account of work sponsored by an agency of the United States Government. Neither the United States Government nor any agency thereof, nor any of their employees, makes any warranty, expressed or implied, or assumes any legal liability or responsibility for the accuracy, completeness, or usefulness of any information, apparatus, product, or process disclosed, or represents that its use would not infringe privately owned rights. Reference herein to any specific commercial product, process, or service by trade name, trademark, manufacturer, or otherwise, does not necessarily constitute or imply its endorsement, recommendation, or favoring by the United States Government or any agency thereof. The views and opinions of authors expressed herein do not necessarily state or reflect those of the United States Government or any agency thereof.

PHOTON AND DIPHOTON PRODUCTION AT CDF AND D0

Presented by Jodi I. Lamoureux
Brandeis University/CDF

For the CDF and D0 Collaborations

ABSTRACT

Measurements of prompt photon production in $\bar{p}p$ collisions at $\sqrt{s} = 1.8$ TeV from the CDF and D0 experiments at Fermilab are presented. The measured inclusive isolated photon spectrum at CDF and D0 are used to test current parton distribution functions and NLO QCD predictions. No new resonance is found in the photon + jet mass spectrum from D0 which is consistent with NLO QCD predictions. The pseudorapidity distribution of the leading jet in photon events at CDF is used to constrain the parton distribution sets while the angular distribution is found to be better explained by a larger Bremsstrahlung contribution. The soft diphoton spectrum is compared to NLO QCD predictions. The diphoton system P_T is found to agree better with the LO shower monte-carlo prediction of Pythia than NLO QCD. Finally, the γ + charm cross section is measured and compared to the LO Pythia prediction.

Prompt photon production is studied at the Fermilab Collider in order to test current parton distribution functions and QCD predictions. At lowest order, the Compton process dominates showing that photons are a direct probe of the gluon distribution in the proton. To test current QCD predictions, comparisons are made between data and NLO calculations. In some cases we find that NLO calculations are insufficient to describe the data well and that effects of higher order QCD processes can be observed as additional transverse momentum (K_T) in the data.

1. Inclusive Isolated Photon Production

1.1. Event Selection and Background Subtraction

To measure prompt photons both CDF and D0¹⁾ employ EM calorimeters segmented into towers in $\eta\phi$ space. The background from neutral mesons π^0 , η and K_S^0 in jets is suppressed by requiring isolated photon candidates; CDF requires less than 2 GeV in a cone of radius 0.7 in $\eta\phi$; D0 requires less than 2 GeV in the annulus between $R = 0.2$ and $R = 0.4$. Both experiments (CDF,D0) require photon candidates to have little hadronic energy (HAD/Total < 11%, 4%), be neutral (no track, dE/dX separation), have good shower profile (strip χ^2 , depth+transverse χ^2), and be central ($|\eta| < 0.9, 0.9$). Cosmic ray muon bremsstrahlung is rejected with a missing E_T cut ($\cancel{E}_T/E_{T\gamma} < 0.8, 0.5$). CDF also requires no extra local energy depositions in a strip chamber greater than 1 GeV, and an event vertex within 60 cm of the center of the detector. Both experiments have three trigger thresholds in E_T . For this analysis CDF uses $0.06 pb^{-1}$ above 6 GeV, $16 pb^{-1}$ above 16 GeV, $19 pb^{-1}$ above 50 GeV and D0 uses $0.014 pb^{-1}$ above 6 GeV, $0.065 pb^{-1}$ above 14 GeV, and $11.4 pb^{-1}$ above 30 GeV. A hardware isolation cut in the CDF trigger makes it possible to acquire more data at low P_T .

After all cuts, a background predominantly from isolated π^0 and η mesons remains. To remove this background one of two methods, a photon conversion probability measure or a photon shower profile measure, are used.¹⁾

The fraction of data which are photons is shown in Figures 1a and 2a as a function of photon P_T . These fractions are used differently in the CDF and D0 analyses. CDF uses a bin by bin background subtraction in P_T whereas D0 uses the functional fit shown to subtract the background contribution. Using the D0 method, the CDF statistical uncertainty is reduced by a factor of ~ 4 . D0 has investigated the shape dependent systematic uncertainty in the fit which is correlated bin to bin, but may vary from the minimum shown at low P_T to the maximum shown at high P_T or vice versa.

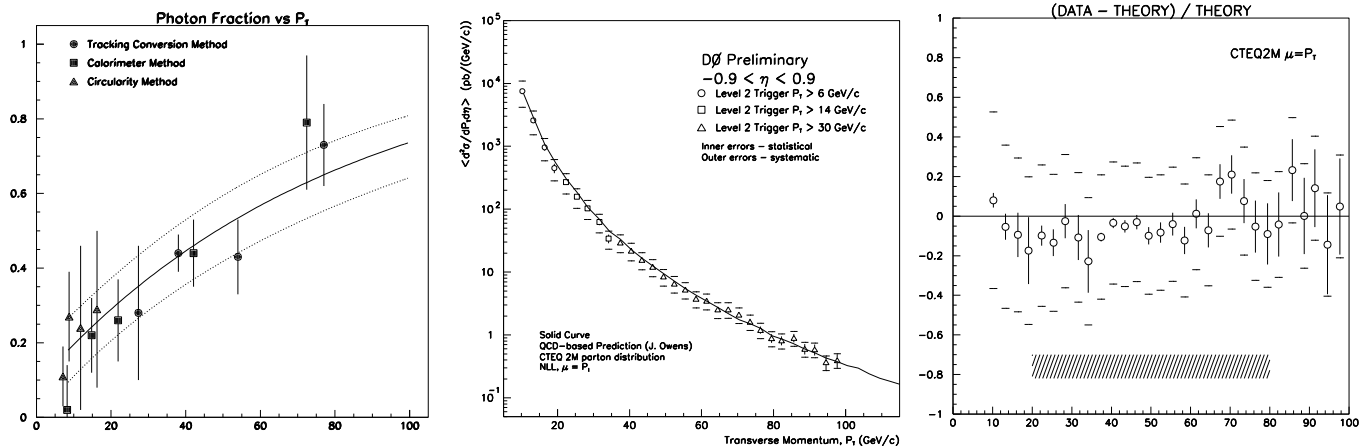


Figure 1: LEFT TO RIGHT a) The fraction of D0 data which are photons. b) D0 inclusive isolated photon cross section c) The fractional difference between the data and NLO QCD prediction.

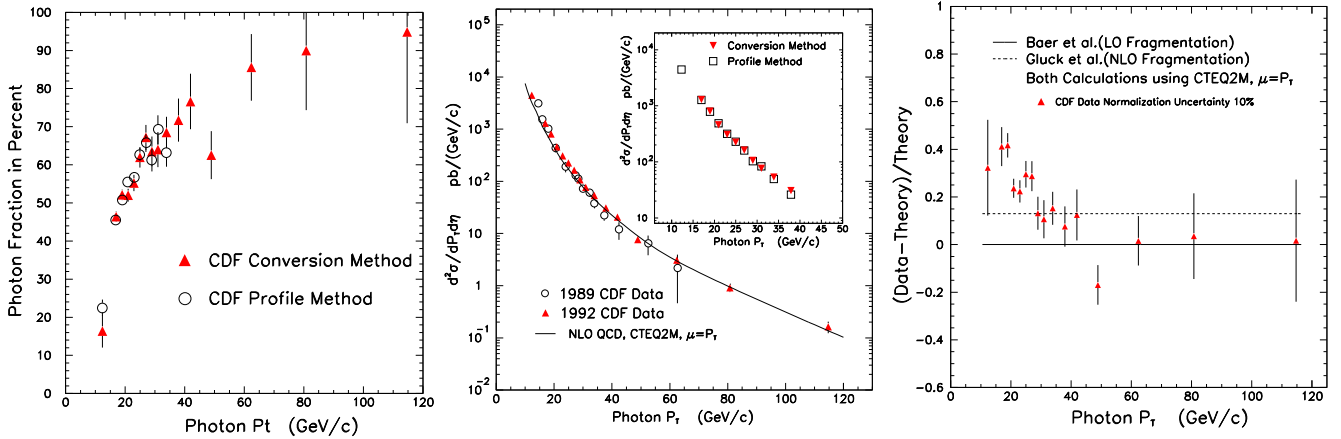


Figure 2: LEFT TO RIGHT a) The percentage of CDF data which are photons. b) CDF inclusive isolated photon cross section c) The fractional difference between the data and NLO QCD prediction.

1.2. Inclusive Isolated Photon Results

The measured inclusive photon cross section from D0 is shown in Figures 1b and 1c. Good agreement is found between data and the prediction ²⁾ of NLO QCD.

The same for CDF is shown in Figures 2b and 2c. Although there is qualitative agreement between data and the NLO QCD prediction over almost five orders of magnitude, the fractional difference between the data and theory show that the data has a steeper slope at low P_T . This result has been previously reported ¹⁾ and it was shown that current parton distributions and QCD scale do not explain the slope of the data. For comparison, the theoretical prediction including a NLO fragmentation function ³⁾ is shown. The data may indicate that events at CDF have more K_T than is currently predicted by NLO QCD ⁴⁾ or that the gluon distribution which has never been directly measured in this x region needs adjusting ($0.0013 < x < .13$).

2. Photon + Jet Mass

The invariant mass spectrum for the photon and lead jet can be used to test QCD as well as search for new mass resonances. Data are selected with $P_T^\gamma > 30$ GeV/c and $|\eta_J| < 3.5$ at D0. All observed jet clusters more than 90° away in azimuth from the photon were summed and the mass shown in Figure 3 is calculated using photon and jet four-momenta. Good agreement is found with QCD and there is no indication of a statistically significant resonance. A previously reported CDF resonance search ⁵⁾ found similar results.

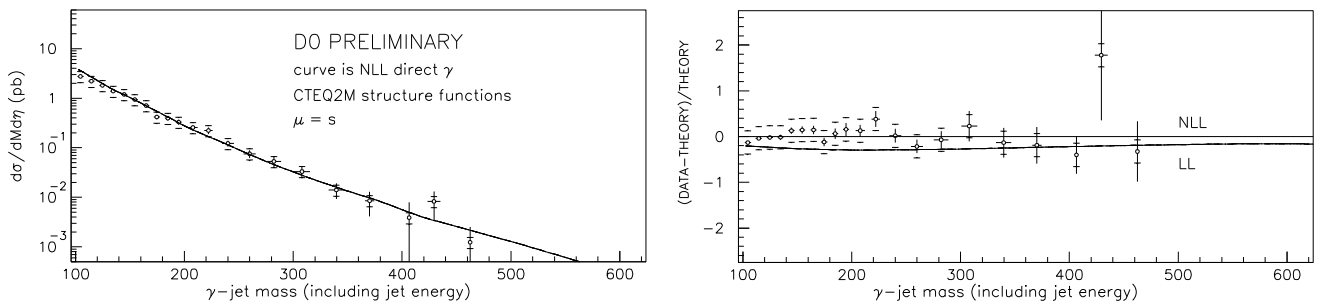


Figure 3: LEFT TO RIGHT a) The photon and jet mass distribution in D0 events (points) compared to NLO QCD (histogram). b) The fractional difference between the data and NLO QCD.

3. Photon + Jet Pseudorapidity

A measurement of the parton distribution functions which is insensitive to K_T comes from the jet pseudorapidity distribution in photon events. The CDF conversion background subtraction method is used for photons in the range $16 < P_T^\gamma < 40$ GeV/c where the jet is required to be back to back with the photon, $150^\circ < \Delta\phi_{\gamma J} < 210^\circ$. All other cuts are the same as for the inclusive spectrum. The $\Delta\phi_{\gamma J}$ cut rejects many two jet events. The pseudorapidity distribution is shown in Figure 4 where data have been corrected for detector resolution based on the results of a monte-carlo simulation. In order to compare the shape of the distributions, the theoretical prediction has been normalized to the first bin of the data. Figure 4b shows that CDF is becoming sensitive to the differences between modern distribution functions.

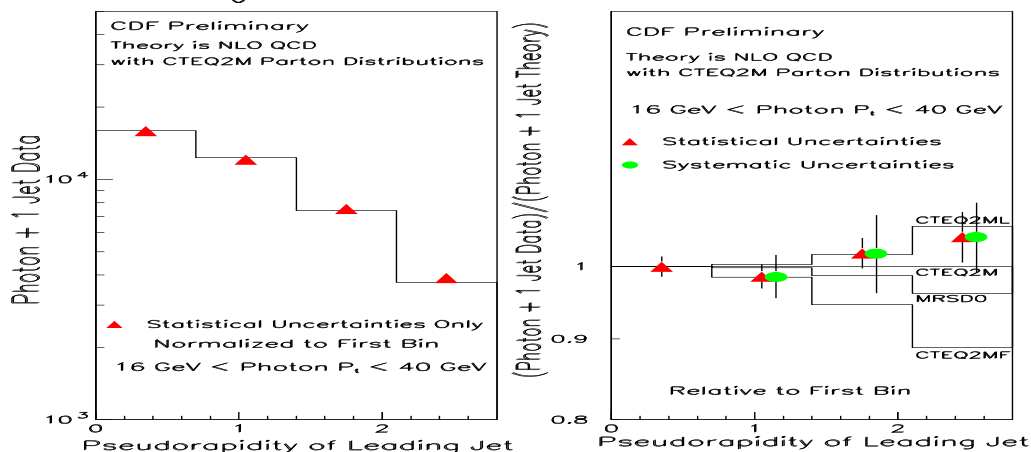


Figure 4: LEFT TO RIGHT a) The jet pseudorapidity in CDF photon events (points) compared to NLO QCD (histogram). b) The ratio of data to NLO QCD (CTEQ2M) and the ratio of various parton distribution sets to CTEQ2M. Statistical and systematic uncertainties are shown separately.

Since the photons in this analysis are restricted to $|\eta^\gamma| < .9$, events with jets at large pseudorapidity are boosted more than events with central jets. Boosted events come from one high x parton and one low x parton. The average low x partons which contribute to each bin in these distributions varies by less than a factor of two whereas the average high x partons vary by more than a factor of five. Since the observed shapes are due to the high x partons which are less sensitive to K_T , this result is essentially independent of K_T .

4. Gauge Boson + Jet $\cos\theta^*$ Distribution

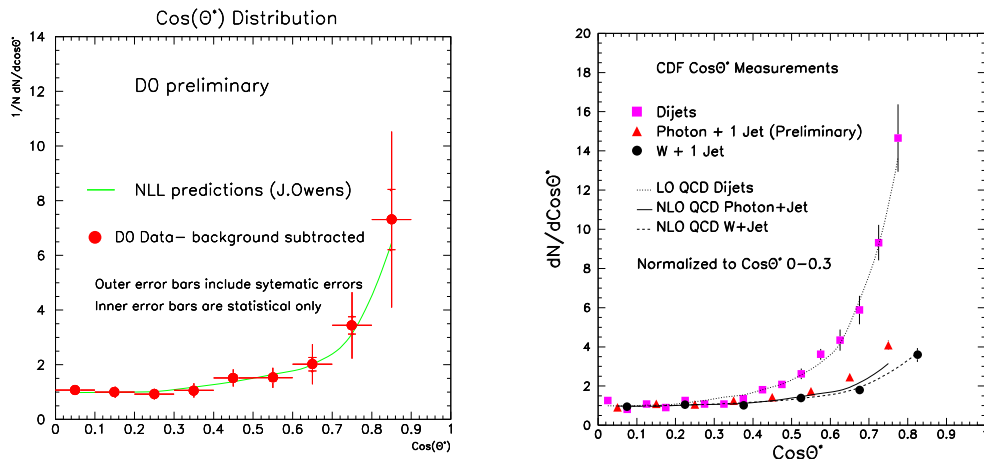


Figure 5: LEFT TO RIGHT a) D0 $\gamma + \text{jet } \cos\theta^*$ distribution. b) CDF angular distributions for dijet, $\gamma + \text{jet}$, and $W^\pm + \text{jet}$ events are compared to QCD predictions.

The $\cos\theta^*$ distribution is very sensitive to the relative contributions of LO and NLO diagrams. At lowest order, u and t channel γ and W^\pm production are achieved most often through the exchange of a spin 1/2 quark which has a $1/(1 - \cos\theta^*)$ dependence whereas jets are most often produced through the exchange of a spin 1 gluon which has a $1/(1 - \cos\theta^*)^2$ dependence. D0 measures the photon $\cos\theta^*$ distribution (Figure 5a) using data from the $P_T^\gamma > 30$ GeV/c trigger. Photons were also restricted to regions of constant acceptance in η^* , η^{boost} , and P^* .⁶⁾ The neutral meson background ($\cos\theta^* < 0.6$) is $\sim 48\%$ of the data sample. The measured angular distribution has been corrected for this background by subtracting the expected contribution of dijets. CDF uses the same photon and jet sample as for the jet pseudorapidity measurement. Events are restricted to regions of constant acceptance.⁷⁾ This is compared in Figure 5b to the previously reported dijet and vector boson results.⁸⁾ The gluon exchange is clearly visible in the dijet data. The photon data is steeper than NLO theory. The W^\pm distribution is flatter than the photon because it is produced more often through the s channel which has no angular dependence.

To investigate the effect of more gluon propagators, CDF compares the photon data to the sum of the NLO QCD prediction and a dijet component (Figure 6a). The best fit for all data is found for 8% more dijet like contribution. It has been suggested that such a contribution may come from NLO photon fragmentation.³⁾ For the perturbative hard radiative case where two jets are observed in the data, there is agreement between data and LO QCD. Figures 6b and 6c show the $\cos\theta^*$ distribution of the photon and lead jet when an additional jet is either FAR ($\Delta\phi_{\gamma J_2} > \pi/2$) or NEAR ($\Delta\phi_{\gamma J_2} < \pi/2$) the photon. The NEAR case is more likely photon bremsstrahlung than the FAR case. The systematic uncertainty for the two distributions is uncorrelated.

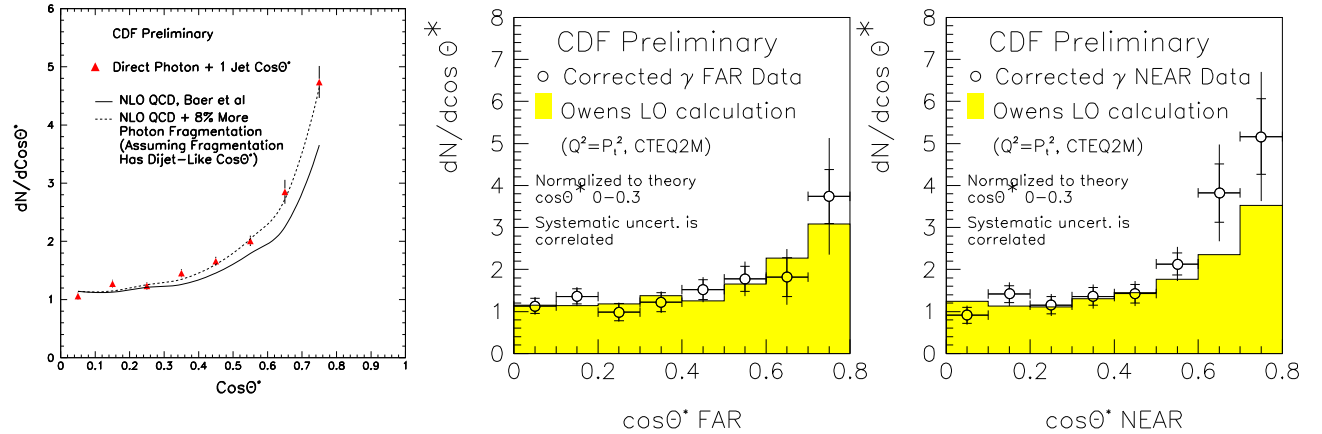


Figure 6: LEFT TO RIGHT a) CDF γ + jet angular distribution with an extra dijet like component. b) CDF γ + lead jet angular distribution in the two jet sample for the FAR region ($\Delta\phi_{\gamma J_2} > \pi/2$) and c) for the NEAR region ($\Delta\phi_{\gamma J_2} < \pi/2$).

5. Diphotons

Measurements of diphotons test NLO QCD⁹⁾ processes which are a background to $Higgs \rightarrow \gamma\gamma$. The CDF high E_T analysis has been previously reported¹⁰⁾ and the new low E_T results are shown in Figure 7. For this analysis, both photons were required to have $E_T > 10$ GeV and satisfy the same cuts as the inclusive photons except that the second photon isolation cut was relaxed to 4 GeV. The E_T distribution of both photons is slightly lower than the previous measurement and is in agreement with NLO QCD. The diphoton system P_T distribution shows that events at CDF have K_T in excess of NLO QCD, but are in agreement with Pythia's shower monte-carlo prediction.

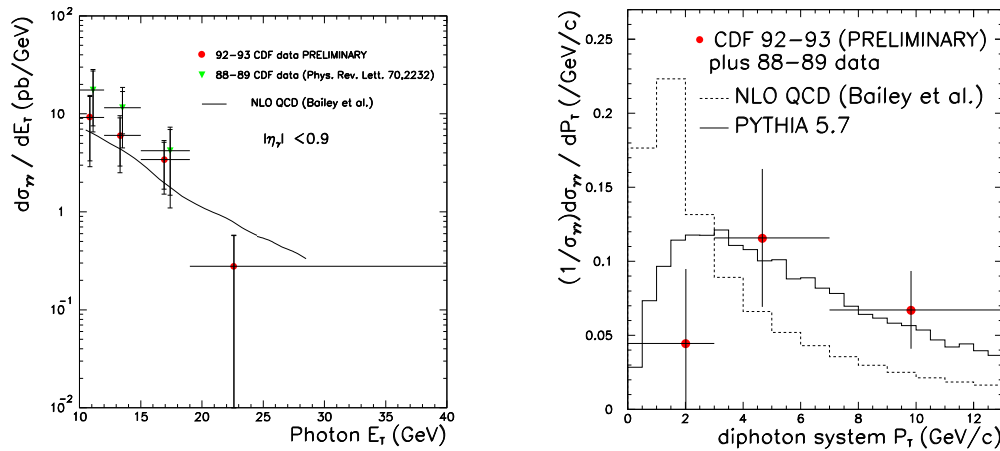


Figure 7: LEFT TO RIGHT a) CDF Diphoton E_T spectrum. b) Diphoton system K_T distribution.

6. γ + Charm Quark Cross Section

The γ + charm quark cross section is measured at CDF in order to understand the charm sea quark distribution at the x range and \sqrt{s} probed by the Tevatron. Two analyses have been completed using the inclusive photon sample described above and further requirements to identify the charm quark. In the first, the charm quark is tagged by a muon ($|\eta^\mu| < 0.6$, $P_T^\mu > 4$ GeV/c). Backgrounds to the muon sample from pion punch-through and decay-in-flight are subtracted. Bottom contamination is subtracted based on the P_T of the muon relative to the nearest jet. The measured cross section in this kinematic region is $(45 \pm 17$ stat ± 11 syst) pb compared to the LO Pythia prediction (MRSD0, $Q^2 = \hat{s}$) of 23 pb. In the second analysis, the charm quark is identified through the reconstruction of the $D^{*\pm}$ particle from the sequential decay to $D^0\pi^\pm$ and $D^0 \rightarrow K^\mp\pi^\pm$ or $K^\mp\pi^\mp\pi^\pm\pi^\pm$. Momentum cuts on the tracks restrict the $D^{*\pm}$ production to $|\eta^{D^{*\pm}}| < 1.2$ and $P_T^{D^{*\pm}} > 6$ GeV/c. The measured cross section in this kinematic region is $(0.48 \pm 0.15$ stat $_{-0.08}^{+0.07}$ syst) nb compared to the Pythia prediction (CTEQ2M, $\mu = P_T$) of .211 nb.

7. Conclusions

Measurements of prompt photon production at the Fermilab Collider provide precision tests of NLO QCD and constrain the gluon distribution of the proton. In some cases we have found that NLO QCD is insufficient to describe the data well. In addition, no evidence is found in the γ + Jet invariant mass distribution for new resonances. The charm cross section is larger than the LO prediction of Pythia.

References

1. F. Abe *et al.* (CDF Collaboration), *Phys. Rev. Lett.* **73**(1994)2662;
S. Fahey (D0 Collaboration), DPF94, Fermilab-Conf-94/323A-E.
2. H. Baer, J. Ohnemus, and J. F. Owens, *Phys. Lett.* **B234**(1990)127
3. Gluck *et al.*, *Phys. Rev. Lett.* **73**(1994)388.
4. J. Huston *et al.*, MSU-HEP-41027, CTEQ407.
5. F. Abe *et al.* (CDF Collaboration), *Phys. Rev. Lett.* **72**(1994)3005.
6. P. Rubinov (D0 Collaboration), DPF94, Fermilab-Conf-94/323B-E.
7. F. Abe *et al.* (CDF Collaboration), *Phys. Rev. Lett.* **71**(1993)679.
8. F. Abe *et al.* (CDF Collaboration), *Phys. Rev. Lett.* **62**(1989)3020;
R. Harris, (CDF Collaboration), Proceedings of the XXIXth Rencontres de Moriond (1994), Fermilab-Conf-94/101-E.
9. B. Bailey, J. F. Owens and J. Ohnemus, *Phys. Rev.* **D46**(1992)2018.
10. R. Blair (CDF Collaboration), DPF94, FERMILAB-CONF-94/269-E.